The NederDrone

A hybrid lift, hybrid energy hydrogen UAV

De Wagter, C.; Remes, B.; Smeur, E.; van Tienen, F.; Ruijsink, R.; van Hecke, K.; van der Horst, E.

DOI
10.1016/j.ijhydene.2021.02.053

Publication date
2021

Document Version
Final published version

Published in
International Journal of Hydrogen Energy

Available online at www.sciencedirect.com

ScienceDirect

journal homepage: www.elsevier.com/locate/he

The *NederDrone*: A hybrid lift, hybrid energy hydrogen UAV

C. De Wagter [1,*], *B. Remes, E. Smeur, F. van Tienen, R. Ruijsink, K. van Hecke, E. van der Horst*

Micro Air Vehicle Lab, TUDelft, Kluyverweg 1, 2629HS, Delft, the Netherlands

HIGHLIGHTS

- Novel versatile hydrogen tail-sitter UAV.
- Powered with hydrogen from a pressure cylinder.
- Fixed-wings give it very efficient flight properties.
- 12 propellers allow vertical take-off and landing even on a moving ship.
- Safe design by making propulsion, energy source, wiring, and flight modes redundant.

GRAPHICAL ABSTRACT

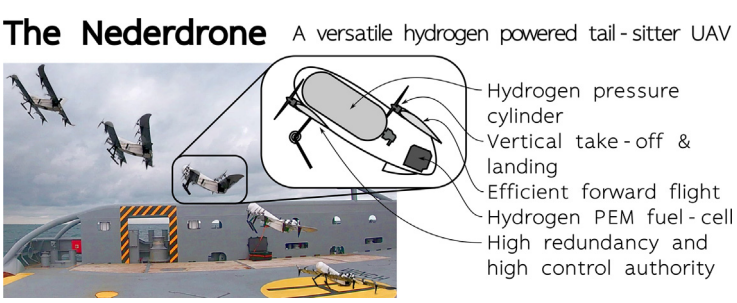

ARTICLE INFO

Article history:
Received 8 November 2020
Received in revised form
4 February 2021
Accepted 6 February 2021
Available online xxx

Keywords:
Polymer electrolyte membrane fuel-cell
Hydrogen
Pressure cylinder
Tail-sitter
Hybrid unmanned air vehicle
Maritime unmanned air vehicles

ABSTRACT

Many Unmanned Air Vehicle (UAV) applications require vertical take-off and landing and very long-range capabilities. Fixed-wing aircraft need long runways to land, and electric energy is still a bottleneck for helicopters, which are not range efficient. In this paper, we introduce the *NederDrone*, a hybrid lift, hybrid energy hydrogen-powered UAV that can perform vertical take-off and landings using its 12 propellers while flying efficiently in forward flight thanks to its fixed wings. The energy is supplied from a combination of hydrogen-driven Polymer Electrolyte Membrane fuel-cells for endurance and lithium batteries for high-power situations. The hydrogen is stored in a pressurized cylinder around which the UAV is optimized. This work analyses the selection of the concept, the implemented safety elements, the electronics and flight control and shows flight data including a 3h38 flight at sea while starting and landing from a small moving ship.

* Corresponding author.
E-mail addresses: c.dewagter@tudelft.nl (C. De Wagter), b.d.w.remes@tudelft.nl (B. Remes).
[1] http://mavlab.tudelft.nl/

https://doi.org/10.1016/j.ijhydene.2021.02.053

Introduction

Unmanned Air Vehicles (UAV) offer solutions in a large variety of applications [1]. While a lot of applications can be performed with current battery technology, for many others the energy requirements cannot be met [2]. In particular, when combined with the requirement to have Vertical Take-Off and Landing (VTOL) capabilities, the traditional efficient fixed-wing aircraft concept is not an option. For these applications, hybrid concepts have been proposed, namely combinations of efficient fixed-wings and hovering rotorcraft. These vehicles combine the most efficient way of flying, namely using fixed wings, with the capability to land vertically.

The most common categories of hybrid lift Unmanned Air Vehicles (UAV) are the tail-sitters, dual-systems, and transforming UAV [3]. Tail-sitters pitch down 90° during the transition from hover to forward flight, and while they have important drawbacks for pilot comfort [4], they have gained a lot of new interest for UAV. They do not require any mechanical reconfiguration and allow the re-use of the same propulsion systems in several phases of the flight [5]. Many different types of tail-sitters exist. They can either be optimized to maximize the hovering efficiency with a single large rotor [6] or to minimize complexity [7]. Other tail-sitters were optimized for maximal redundancy [8] or were given re-configurable wings to minimize sensitivity to gusts in hover [9].

The second category is formed by dual-systems like quadplanes. These UAVs contain a complete hovering vehicle combined 'in-plane' with a separate fixed-wing vehicle. Both parts are typically operated separately [10].

The last category consists of transforming vehicles that try to re-use propulsion systems in hover and forward flight by either tilting the entire wings with respect to the fuselage [11] or by only tilting the propulsion system [12].

These hybrid concepts increase the endurance of UAV while maintaining the often crucial ability to hover and land vertically. Now, despite large improvements in battery technology and drone technology, energy storage is the biggest bottleneck for the endurance of UAV. Recent lightweight robust fuel-cell technology advancements [13] have led to increased interest in using them in UAV applications [14–17].

Fuel-cells can be divided into five types: alkaline [18], Polymer Electrolyte Membrane (PEM) [19], phosphoric acid [20], solid oxide [21], and molten carbonate batteries [22]. The most suitable for portable micro-systems is the PEM [23] as it can work at room temperature, has a small size, is lightweight, and is anti-aging.

PEM fuel cells can be powered by fuels like liquid methanol [23] or hydrogen [24].

If storage of hydrogen was not such a challenge [25], hydrogen would be ideal as a synthetic fuel because it is lightweight, highly abundant and its oxidation product is environmentally benign. Moreover, the hydrogen to electricity cycle is bi-directional [26]. Hydrogen can be generated in a variety of ways even without generating COx [27]. It can be generated off-grid [28]. And recent research even addresses the generation of hydrogen without the need for rare and expensive platinum (Pt) [29] nor Ru [30] by using hybrid nanoplates as catalytic material instead [31].

Although hydrogen-only flight is the most efficient solution [32], in several hydrogen-powered UAVs the fuel-cell power had to be complemented with batteries [33] since developing small reliable membranes for power-hungry UAV can be a challenge [34]. Hovering requires a higher power density than forward flight [3]. Hydrogen fuel-cell powered quadrotors have been developed in the last decade [15], but their flight times have never reached the endurance seen in fixed-wings.

This is why so many fixed wing hydrogen UAVs have been proposed like the 16 kg 500 W demonstrator from Ref. [35] in 2007, the 1.5 kg 100 W UAV from Ref. [15] in 2012, the 11 kg 200 W from Ref. [16] in 2017 to the 2020 6.4 kg 250 W [17].

As even hydrogen's energy storage capacity is limited, the combination of hydrogen power with solar power has also been investigated [36], which effectively helped to double their flight time in ideal conditions. This combination has also been proposed to cross the Atlantic [37], but requires flight efficiencies currently only seen in fixed-wing aircraft. Therefore the mainstream solution is a combination of battery power for high demand situations and hydrogen power for endurance. This combination is further referred to as hybrid energy [38].

To combine the advantages of hybrid lift UAV with those of hybrid energy from batteries and hydrogen fuel-cells, a new concept is developed called: the *NederDrone*.

Section 2 investigates the selected type of fuel-cell and safety aspects of flying with hydrogen. Section 3 explains the design choices of the hybrid UAV built around the fuel-cell system. Section 4 describes the essential aerodynamic properties. Section 5 explains the hybrid power wiring and dual control bus of the *NederDrone*. Section 6 explains the control. Section 7 shows actual test flight data. Finally Section 8, 9 and 10 give a discussion, conclusions, and recommendations respectively.

Selection of the hydrogen systems

Hydrogen-powered fuel-cells form an attractive solution for sustainable aircraft if the remaining technological problems can be solved [39]. The following sections will address the selection of the fuel-cell, the selection of the fuel storage solution, and its safety considerations.

Fuel-cell

The three most common fuel-cells used to power UAVs are: 1) hydrogen PEM fuel-cells, 2) direct methanol PEM fuel-cells, and 3) solid oxide fuel cells [40]. But the availability of ready to use systems at the time of selection also plays an important role. Although PEM fuel-cell efficiency drops with altitude [19,41], and their membrane must be re-humidified to unlock their full power when not used for a few days [42], their small size and weight form an attractive choice for UAV. Two options within the power range from 300 W to 1000 W were available, namely PEM fuel-cell systems from Intelligent Energy[2] (**IE**) and HES Energy Systems[3] (**HES**) (See Table 1).

[2] http://www.intelligent-energy.com
[3] https://www.hes.sg/

Please cite this article as: De Wagter C et al., The *NederDrone*: A hybrid lift, hybrid energy hydrogen UAV, International Journal of Hydrogen Energy, https://doi.org/10.1016/j.ijhydene.2021.02.053

Table 1 – Available fuel-fell power P, system maximum power P_{max}, number of lithium cells, efficiency ζ and pressure reduced weight $W_{p.r}$.

Unit	P [W]	P_{max} [W]	Lipo [cell]	ζ [%]	W [kg]	$W_{p.r}$ [kg]
HES	250	250	6	50%	0.73	0.14
	500	500	7	52%	1.4	0.14
IE	650	1000	6	56%	0.81	0.14
	800	1400	6	55%	0.96	0.14

the combined system to deliver 1400 W of peak power for a short time.

Hydrogen storage

At room temperature, the main two options to store hydrogen are as a pressurized gas in a pressure cylinder, or as a chemical solution that releases hydrogen [43]. Sodium borohydride ($NaBH_4$) is often used in UAV and portable applications as a hydrogen source to power PEM fuel-cells [24,44,45].

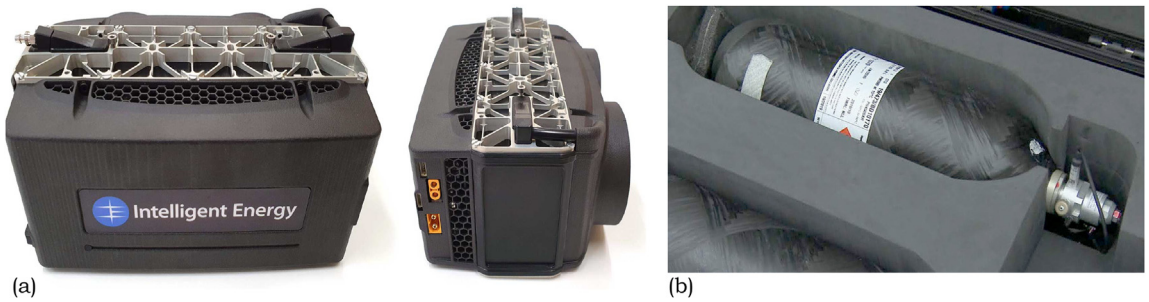

Fig. 1 – Intelligent Energy 800W fuel-cell system with dual fan and 6.8 L 300 bar CTS light Type-4 pressure cylinder in a certified transport case.

The **IE** 800 W air-cooled PEM fuel-cell running at ambient temperatures was selected (See Fig. 1a), which is packaged as a small light-weight cost effective and robust system. It runs at the easily available 6-cell lithium output voltage and—at the time of selection—had the better hydrogen efficiency and weight efficiency of the two.

The Lower Heating Value (LHV) efficiency Eff_{PEMFC} of the 800 W system is between 53% at 800 W and 56% at 700 W.[4] The fuel consumption ff_{H_2} in g/h at the predicted forward flight conditions of 600 W average power then becomes:

$$ff_{H_2} = \frac{P_{mean}}{E_{specific_{H_2}} \cdot Eff_{PEMFC}} \quad (1)$$

A hydrogen LHV of 33.3 W h/g is used in further computations. This results in a fuel consumption (1) of not more than 34 g/h at 600 W average power and up to 45.3 g/h at full power. To fly at least 3 h at maximum fuel-cell power—to also deliver payload power and be able to climb, hover and recharge hover batteries in-flight—about 140 g of hydrogen would be desired.

The corresponding Intelligent Energy Transportable Pressure Equipment Directive (TPED) regulator is 0.28 kg, 40 by 35 mm (diameter x length), 20–500 bar 'in' and 0.55 bar 'out' and is equipped with an electronic shut-off valve, pressure sensors and a standard 8 mm Pre-Charged Pneumatic (PCP) fill port. The fuel-cell system weighs 0.96 kg and measures 196 by 100 by 140 mm. It's output voltage ranges from 19.6 V to 25.2 V. It is equipped with a 1800 mA h 6-cell lithium-polymer auxiliary battery of 0.3 kg which enables

The downside of pressure cylinders is that they weigh much more than the hydrogen inside them [46]. But because of sustainability, overall system weight, off-grid recharge options [47], price, and availability, the choice was made to use pressure cylinders.

The mass of hydrogen m_{H_2} based on the cylinder volume V and pressure p in flight conditions is fitted as[5]:

$$m_{H_2} = (-0.00002757p^2 + 0.074969p + 0.6187) \cdot V \quad (2)$$

It should be noted that the actual value varies with temperature, and is not included in this fit. At 300 bar, values change from 20.7 g/L at 25 °C to 21.2 g/L at 15 °C and a 25 °C drop in temperature leads to a 7.8% increase in hydrogen per liter. In this paper, the more pessimistic values at 25 °C are used. Fig. 2 shows an overview of available cylinder options. The cylinders are compared with respect to the mass of hydrogen they can contain compared to the total cylinder mass called $wt\%H_2$. The original data used to compute this $wt\%H_2$ can be found in A. This shows that, at the time of selection, the cylinders with the best $wt\%H_2$ are the HES A-Series and F-Series.

Unfortunately, due to price, availability, and availability of EU certification, these options were not yet available. The selected cylinder is the 6.8 L Composite Technical Systems (CTS) Polyethylene Terephthalate (PET) Liner Type-4 cylinder.[6] This is the heaviest cylinder that still fitted in the weight budget of the roughly 10 kg UAV. The graph does however illustrate that doubled specific hydrogen weights can be

[4] https://www.intelligent-energy.com/uploads/product_docs/61126_IE_-_Cylinder_Guide_May_2020.pdf

[5] https://h2tools.org/hyarc/hydrogen-data/hydrogen-density-different-temperatures-and-pressures

[6] http://www.ctscyl.com/prodotti/h2/cts-ultralight-6-8l-300-bar-h2

Please cite this article as: De Wagter C et al., The *NederDrone*: A hybrid lift, hybrid energy hydrogen UAV, International Journal of Hydrogen Energy, https://doi.org/10.1016/j.ijhydene.2021.02.053

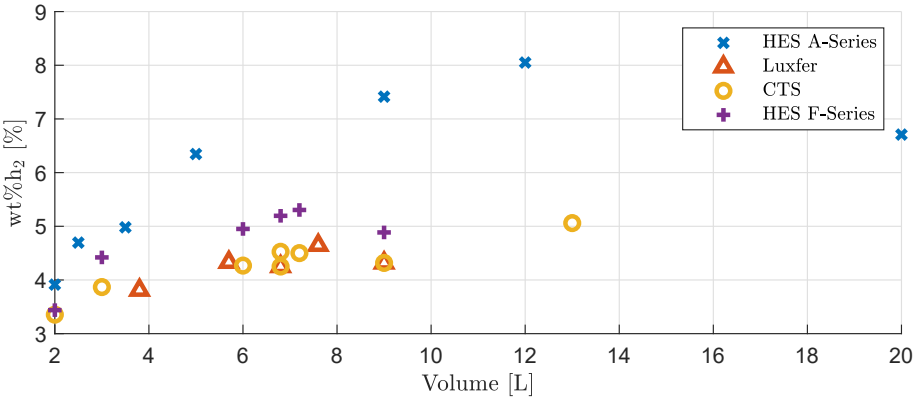

Fig. 2 – Overview of the specific hydrogen weight *wt%H₂* for various cylinders that were available at the time of selection.

expected soon. A picture of the selected cylinder can be found in Fig. 1b.

Safety of handling pressurized hydrogen

Hydrogen gas is flammable in concentrations from 4% up to 75% when mixed with air and burns optimally at a concentration of 29%. It has a self-ignition temperature 585 °C, but a very low required ignition energy of 17 μJ. Human body models show that a person without static protection can easily cause a 40 mJ discharge. To avoid ignition, anti-static shoes and clothes are therefore required when leakages are expected, for instance during filling. Refueling should be done at temperatures in between −20 °C and 40 °C to stay within cylinder's limitations. Hydrogen is roughly 14 times lighter than air and therefore easily gets trapped inside rooms and ceiling cavities. The area where hydrogen is used should be well ventilated as per *ATEX 153* and for ignition analysis, one should refer to *EN1127-1*. At room temperatures, hydrogen is converted to ortho-hydrogen, and no significant heating effect is to be expected when depressurizing it. When assembling a UAV, applicable regulations include the *EU 94/9/EC* (*ATEX 114*) and *ISO 15196* for material properties and their degradation in the presence of hydrogen [48].

Concerning the field of pressure tank rupture analysis, a lot of research has already been done, but most research has been focusing on metal cylinders used for a variety of gasses like Compressed Natural Gas (CNG) [49]. For composite high-pressure cylinders, models and methods have been developed and validated [50], but these do not show all risks of hydrogen cylinder failures.

Actual crush tests of composite hydrogen cylinders have been performed [51] to simulate a car crash. But they used mainly cylinders with aluminum liners (type 3A/B). The blast from hydrogen cylinders exposed to vehicle fires was also investigated [52]. They suggest that the blast from a cylinder failure through fire (with combustion) can throw debris up to 80 m, but also shows that 35 m would be a no-harm distance for the shock-wave of a 12 L 700 bar cylinder.

The selected cylinder was tested by the manufacturer according to the *NEN-EN12245+A1*. But since no data were available about the safety of the combined cylinder and pressure regulator, a drop test was organized that simulated the fall on the metal deck of a ship. While this does not represent the worst-case scenario of a crash involving hydrogen, it does address the operational scenario in which the hydrogen drone moves away from the ship as soon as possible after take-off and only moves over the ship at low speed and low altitude upon landings. The test was performed according to the *STANAG 4375*. The cylinder was dropped from a 12 m high tower on a metal plate on top of a concrete floor while filled with about 140 g of hydrogen (285 bar). High-speed camera footage was made and the post-impact damage was assessed. The metal regulator broke which resulted in a leak. After a few minutes, all hydrogen had escaped and the cylinder was inert. No combustion occurred.

Design of the hybrid lift UAV

After the selection of the fuel-cell system and hydrogen storage, a UAV was designed around it from the ground up. Fitting a hydrogen cylinder and fuel-cell in a hybrid UAV poses specific constraints [14,15,38]. The large and bulky cylinder highly influences the aerodynamic shape. To cool the fuel-cell and remove the formed water vapor, sufficient airflow through the fuel-cell radiator is important. The relatively large weight of the energy supply and payload combined with the weight of the propulsion needed to hover poses strict limitations on structural weight. And flying with pressure cylinders and expensive equipment comes with redundancy requirements. This section will discuss these challenges.

Hybrid lift UAV concept trade-off

First, a trade-off is made between the three main classes of hybrid lift UAVs. The dual-system VTOL UAV like quad-planes have a separate propulsion system for hover and forward

Please cite this article as: De Wagter C et al., The *NederDrone*: A hybrid lift, hybrid energy hydrogen UAV, International Journal of Hydrogen Energy, https://doi.org/10.1016/j.ijhydene.2021.02.053

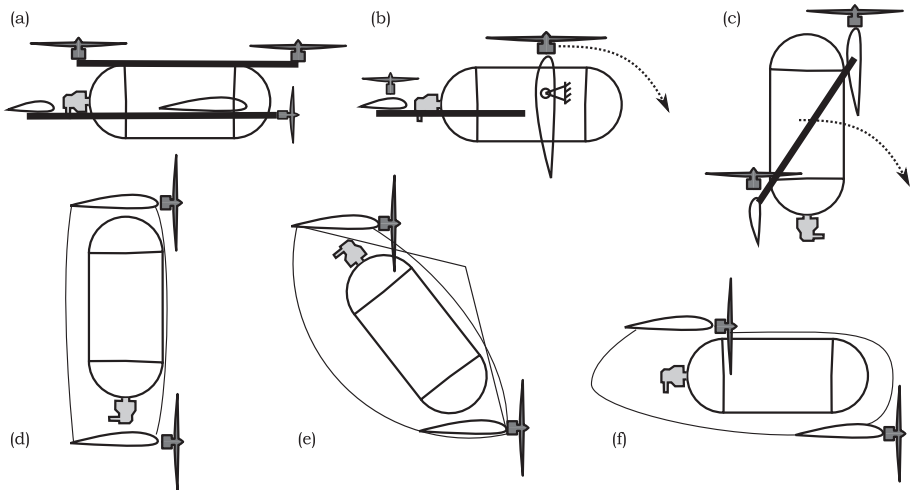

Fig. 3 – Hybrid lift UAV concepts around a hydrogen cylinder and multiple cylinder orientations.

flight (Fig. 3a). To minimize weight, a minimalist hover system is often used as this is only dummy weight during the largest part of the flight. The hover propulsion blows perpendicularly to the wing and therefore needs additional arms to support the motors at a distance from the wing, which also adds weight and drag in forward flight. The tilt-wing (or tilt-motor) concept (Fig. 3b) has a mechanism to rotate the entire wing, thereby removing the need for separate motor support arms and re-using part of the propulsion from hover in forward flight. The downsides are increased mechanical complexity, higher mechanical weight, and the control complexity of flying with a changing morphology. A tail-sitter option shown in Fig. 3c, re-uses the same motors in both flight regimes while minimizing mechanical complexity. The propulsion can be attached to the wing, which is already designed to carry the weight of the vehicle and this reduces overall structural weight. As the vast majority of the flight is typically in forward flight, the propulsion can be optimized for this phase. The drawbacks are that the UAV must pitch down 90° during the transition and therefore passes through the stall regime of the wing. Moreover, the cylinder is vertical after landing which makes it prone to tipping over, especially on moving platforms like ships.

To minimize structural weight and complexity while re-using the hover propulsion in forward flight, the tail-sitter concept was selected for the *NederDrone*.

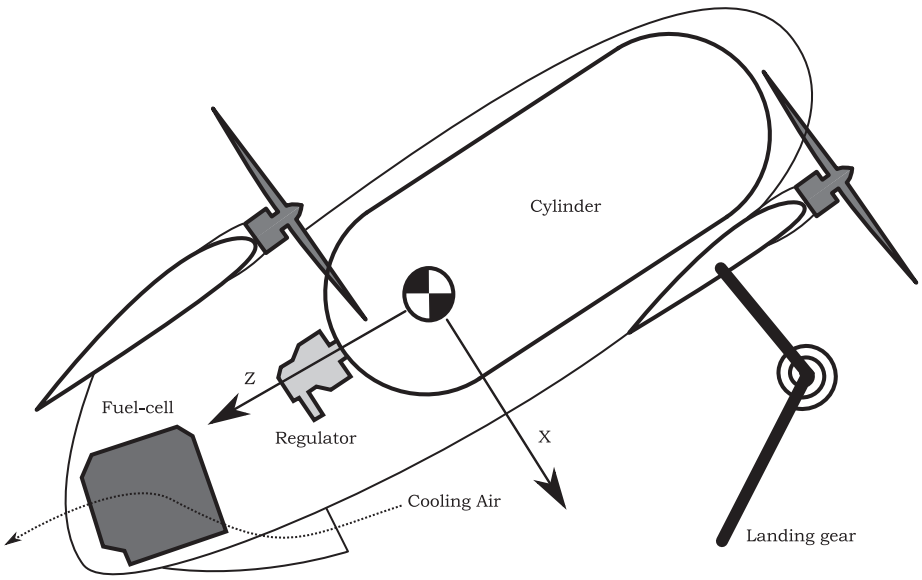

Fig. 4 – The *NederDrone* concept: a *drop-down* tail-sitter with an in-flow oriented hydrogen pressurized cylinder, rear-mounted fuel-cell with bottom cooling airflow vent, low front-wing, and high tail-wing.

Please cite this article as: De Wagter C et al., The *NederDrone*: A hybrid lift, hybrid energy hydrogen UAV, International Journal of Hydrogen Energy, https://doi.org/10.1016/j.ijhydene.2021.02.053

Cylinder placement into the UAV

Within the class of tail-sitter UAVs, three variables form a trade-off for the orientation of the cylinder: drag, ground stability, and control authority in hover. The best control authority in hover is achieved by maximizing the distance between the motor center-lines (Fig. 3d). With this setup, larger control moments can be created through differences in thrust. After landing the cylinder lies flat and stable on the ground. But this configuration has the highest fuselage drag in forward flight as the frontal surface is determined by the cylinder surface in the length direction. Moreover, the wings are then placed on top of each other, which results in an aerodynamically unstable aircraft in forward flight without an S-shaped airfoil or significant wing sweep angle.

Previous work [8] made a compromise and placed the cylinder at a negative 30° angle with the incoming flow (Fig. 3e). The presumed advantages during the landing phase to slowly roll down were found to be insufficient and a landing gear was still needed to protect the propellers. Moreover, the design goal of staying below 600 W in forward flight could not be achieved. Therefore the cylinder was placed completely in-line with the flow as in Fig. 3f. This associated reduction in drag is also important to increase the maximal forward flight speed.

Sizing the wings, stabilizer, and fuselage

The next step of the hybrid lift UAV design is the sizing of the wings, horizontal stabilizer and fuselage, to achieve stable forward flight characteristics. The selected concept has the cylinder and the fuel-cell placed in-line to minimize drag, which makes the longitudinal distribution of mass in the length of the fuselage significant. To improve the damping of the short period pitch motion in forward flight, either a large elevator or a long fuselage is required [53]. But since this is a hybrid UAV, a long fuselage conflicts with the ground stability requirement after landing, as a long narrow tail-sitter is at high risk of tipping over.

The combined requirements are addressed by giving the *NederDrone* a short fuselage and a tandem wing configuration. The tandem wing has the best pitch damping for a given fuselage length [53]. Moreover, it has a shorter wingspan for a given amount of wing area at a given aspect ratio compared to a conventional large main wing and a small horizontal stabilizer. These shorter wings help to cope with higher perturbations in hover, as they provide less leverage to perturbations.

Ground stability

Since the pressure cylinder is placed in the direction of the airflow during forward flight, it is upright during the landing. The stability of this long upright vehicle after landing must nevertheless be guaranteed, even on a moving platform like a ship.

Inspired by Ref. [8], illustrated in Fig. 3f, the option was investigated to slowly *drop-down* the nose after landing, by using the hover propellers. Once the hover propellers start to point forward beyond a certain angle, the ground friction is overcome and the drone would start to slide forward. At this point, the thrust is cut off and the nose drops down. To allow this, sprung landing gear was added which could absorb the last part of the drop. The result is a UAV which lies stable on the ground after landing.

To further minimize the impact of the landing, the center of gravity was moved backward by choosing a canard configuration with the largest wing at the back. This places the center of gravity much closer to the ground while in hover. The resulting landing sequence is shown in Fig. 6c.

Take-off

In tail-sitter UAVs, the ground stability requirement is conflicting with the vertical take-off requirement of the tail-sitter. Since the UAV is sitting in a 60° nose down from hover, this affects the vertical take-off. However, test flights showed that even in worst-case 'no-wind' conditions the UAV only slides less than a foot before taking off as shown in composite image Fig. 6a. With more wind the sliding becomes neglectible Fig. 6b. The high thrust to weight, the ground effect of the propeller flow over the wing squeezed between the wing and the ground, and the spring in the landing gear makes the *NederDrone* take-off on the spot into what will be referred to as an angled take-off.

The resulting hybrid-hybrid vehicle designed around a pressure cylinder has minimal drag in forward flight, has tandem wings that also serve as structural support for the 12 propellers, does not require mechanical reconfiguration but uses its redundant propulsion in both flight regimes, can take-off and land vertically and is stable on the ground before take-off and after landing.

Aerodynamics

Once the general concept shape was determined, the aerodynamics properties were designed and tested. The airfoil for the wings has been chosen to yield a good compromise between 'gentle stall' and 'low drag throughout the lift curve' using the *XFoil* module within XFLR5[7]. The resulting airfoil is based on a *MH32* airfoil but was modified to allow construction from Expanded Polypropylene (EPP). Wind-tunnel measurements were performed in the TUDelft Open Jet Facility (OJF) [54], in which the full-scale *NederDrone* was tested.

The lift and drag forces were measured at different speeds and angles of attack α from zero to over 60°. The resulting lift curve is shown in Fig. 5 and confirms that the airfoil has gentle stall properties but also that the front and back wings of the tandem aircraft are properly placed not to cause detrimental interactions with each other. These two properties are very important for flight control as abrupt changes highly affect the control of the platform.

[7] http://www.xflr5.tech/.

Please cite this article as: De Wagter C et al., The *NederDrone*: A hybrid lift, hybrid energy hydrogen UAV, International Journal of Hydrogen Energy, https://doi.org/10.1016/j.ijhydene.2021.02.053

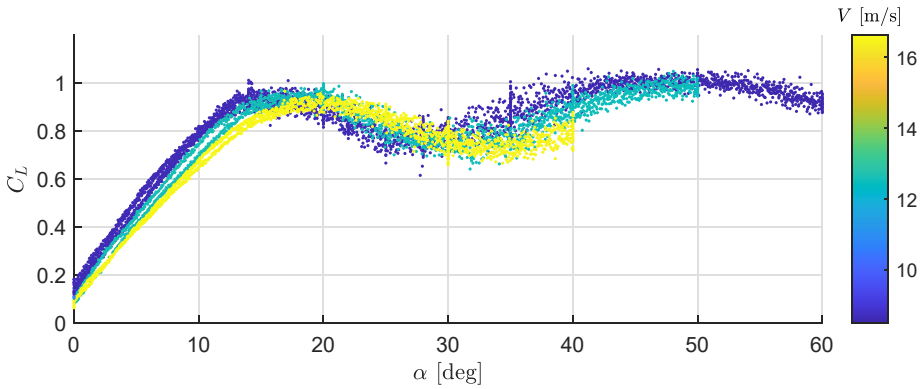

Fig. 5 – Lift curve (lift coefficient C_L in function of angle of attack α) of the *NederDrone* as measured during wind tunnel testing. The stall starts at about 15° but is very gentle. This is important during the transition phase of the tail-sitter UAV as abruptly changing lift forces complicate the control.

Electronics

With the concept design to fit the available fuel-cell power in forward flight finished, the required power to hover was analyzed.

Hybrid electric power

Hovering a roughly 10 kg platform in gusts while the propulsion is optimized for the forward flight regime is taking more than the 1400 W maximum of the selected fuel-cell system. To complement the fuel-cell during the short high power phases, high C-rating lithium polymer batteries are added to the *NederDrone*. This is typically done with two DC-DC converters and a power management system. This allows to apply various types of intelligent power management strategies, for instance, based on fuzzy logic [55]. But even with state-of-the-art Gallium Nitride (GaN) technology, the mass of DC-DC converters is not negligible [56]. To avoid this heavy power electronics to merge both energy sources, a passive approach is designed where both power sources are connected in parallel. The company proprietary DC-DC converter inside the **IE800** fuel-cell system is tuned to act as a 25 V constant voltage source when the used power is less then 800 W, and as an 800 W constant power source when the battery voltage drops below 25 V.

The fuel-cell provides a nominal output voltage of 25 V, which drops when the load increases. The six-cell lithium-polymer battery recommendations state that they can safely be charged up to 25.2 V, which is compatible with the fuel-cell voltage range including a safety margin of 0.2 V to prevent over-charge. To minimize weight, the batteries are therefore connected directly to the motors in parallel to the fuel-cell. To prevent that the hover batteries would feed current into the fuel-cell, the fuel-cell current is run through a pair of *SBRT15U50SP5-13* 15 A continuous power diodes at each motor. This allows the very high currents to go from the lithium battery directly to the Electronic Speed Controller (ESC) without loss and allows the fuel-cell to re-charge the batteries to about 25 V minus the diode forward drop voltage of about 0.2 V in cruise conditions. To minimize power loss, maximize redundancy and distribute heat production, two diodes are used per motor, which results in lower current per diode and thereby also lower forward voltage V_F. This means the lithium-polymer batteries are charged up to about 24.8 V

Fig. 6 – Composite image of the *NederDrone* take-off with 2 m/s (a) and 7 m/s wind (b) and a landing sequence (c).

Please cite this article as: De Wagter C et al., The *NederDrone*: A hybrid lift, hybrid energy hydrogen UAV, International Journal of Hydrogen Energy, https://doi.org/10.1016/j.ijhydene.2021.02.053

which corresponds to at least 95% full. The fuel-cell and lithium batteries can thus safely be placed in parallel without the need for heavy power electronics nor additional charging circuits.

The hover batteries have been selected to provide 800 W for 30 min in case the fuel-cell would fail in-flight. This allows the UAV to safely return and land. The selected batteries are four *Extron X2* 4500 mA h 6S 1P lithium-polymer batteries with a nominal voltage of 22.2 V and a discharge rate of 25C–50C. They contain just under 100 W h of additional energy at 640 g each and can supply 90 A continuous current and 180 A burst current, which is more than sufficient to handle the largest peak currents. The four batteries are placed as close as possible to the four wings to supply the 3 motors on each wing through short high power wires for minimal loss.

Redundant control of 20 actuators using aerospace CAN

For redundancy and structural weight distribution purposes the *NederDrone* has twelve motors. Moreover, it has 8 aerodynamics flaps. To reduce wiring and connector failures and create a system that is still able to fly even if any of the wires would fail, the power and control wires need to be duplicated. This would lead to 24 control wires going to the 12 motors, excluding the motor status feedback wires and dual power bus and 16 additional control wires to servos. To reduce this large amount of wiring and weight, the *NederDrone* uses a control network instead. The Controller Area Network (CAN) is an automotive industry technology that has been proposed as a low-cost solution in several aerospace applications [57]. The increasingly popular [58] *UAVCAN*[8] implementation was selected with custom messages. The resulting system is a setup where any control or power wire can be cut without dramatic consequences while the weight and complexity are kept to a minimum.

Flight control

Challenges of tail-sitter control

The flight control of the *NederDrone* tail-sitter UAV poses several special challenges. First, the lift and moments generated by the wings are hard to model at large angles, which occurs when tail-sitters fly slowly and the nose starts to point upwards. Sudden changes in the aerodynamic forces and moments can occur when the flow over the wings suddenly stalls or re-attaches, and this requires fast and powerful control actions to compensate. In hover, the large exposed up-pointing wing surfaces make tail-sitters susceptible to wind gusts, which need to be compensated by the controller. Moreover, specifically to the *NederDrone* with its tandem-wing configuration, the slipstream from the front wing can hit the back wing at certain attitudes. This is expected to produce a complex interaction at certain angles of attack (consider Fig. 4 and imagine a horizontal velocity to the right), which would be hard to predict, and hereby difficult for the controller. Finally, the experimental nature of the project required a control method that could be easily adapted to changes made to the platform, without needing new wind tunnel tests.

To cope with these challenges, an Incremental Nonlinear Dynamic Inversion (INDI) controller was selected as it does not rely heavily on aerodynamic modeling but uses a sensor-based approach to identify external forces. INDI has been successful implemented on tail-sitters with similar challenges like the Cyclone tail-sitter UAV [7].

Cascaded INDI control

INDI is a control method that makes use of feedback of linear and angular acceleration to replace much of the modeling needs since these signals provide direct information on the forces and moments that act on the vehicle [59]. The angular acceleration can be obtained through differentiation of the gyroscope signal, and the linear acceleration is directly measured with the accelerometer. To ensure a timely and well-scaled response to these external forces, INDI does require the modeling of the actuators' responses and their control effectiveness. Based on the difference between desired and measured linear and angular acceleration, control *increments* are then calculated using this control effectiveness. Because disturbances are directly measured with the accelerometer and the gyroscope, they can be counteracted very effectively. The disturbance rejection properties of INDI have been shown theoretically and experimentally in previous research [60,61] and its successful implementation on a tail-sitter has been detailed in Ref. [7].

The general structure of the controller is given in Fig. 7, in which ξ is the position, η is the attitude, and ω the angular rate of the vehicle. The control moments are denoted by L, M and N, the total thrust is T, and the commands to the servos and motors is u. Signals that are filtered with a low pass filter have a subscript f.

The controller is split into an outer-loop that controls the position and an inner loop that controls attitude. Both start with a linear controller to generate the desired reference signal; linear acceleration $\ddot{\xi}_r$ and rotational acceleration $\dot{\omega}_r$ respectively. These signals are then compared with the respective filtered measurements $\ddot{\xi}_f$ and $\dot{\omega}_f$. The INDI blocks then compute increments in actuator deflection using the respective actuator effectiveness and dynamics that should exactly cancel the errors in linear or rotational acceleration [60].

Structural modes

One particular property of the tandem-wing tail-sitter UAV which was found during flight testing, is the relatively low frequency of some of the structural modes—in particular the longitudinal torsion mode. This is due to the large spread in mass over the wings, the relative flexibility of the wings combined with the relatively low torsional stiffness of the fuselage. To avoid interaction between the controller and the structural modes, the common procedure in aerospace is to make sure that the controller has a sufficiently small open-loop gain at the structural resonance frequency [62].

[8] https://uavcan.org/.

Please cite this article as: De Wagter C et al., The *NederDrone*: A hybrid lift, hybrid energy hydrogen UAV, International Journal of Hydrogen Energy, https://doi.org/10.1016/j.ijhydene.2021.02.053

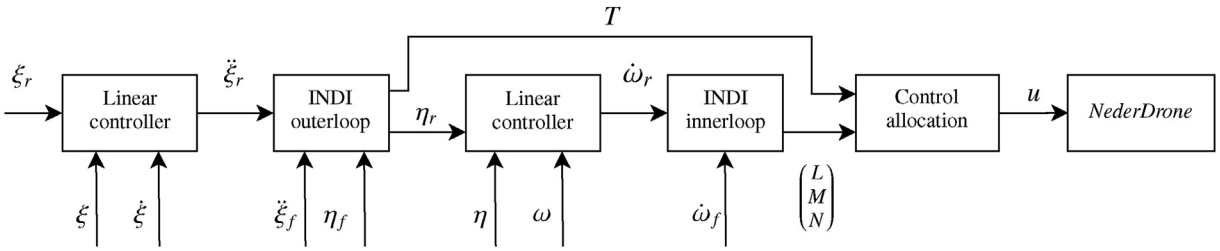

Fig. 7 – A schematic overview of the cascaded INDI control approach used in the *NederDrone*. ξ is the position, η is the attitude, and ω the angular rate of the vehicle.

This can be achieved by including a low pass or a notch filter on the relevant feedback signals $\ddot{\xi}_f$ and $\dot{\omega}_f$. For the INDI inner loop, there is already a low pass filter, since the angular acceleration signal is typically noisy due to high-frequency vibrations coming from the motors. Though including a separate notch filter to dampen the structural mode could result in an overall lower phase lag, this also requires knowledge of the frequency of the structural modes. To minimize complexity, the cutoff frequency of the second-order Butterworth low pass filter that was already in place was set to 1.5 Hz for the pitch rate and roll rate, and to 0.5 Hz for the yaw rate and linear acceleration. It should be noted that these filter cutoff frequencies are relatively low, and lead to reduced disturbance rejection performance. Increasing the stiffness of the platform and hereby the frequencies of the structural body modes can therefore improve the disturbance rejection.

Disturbance rejection

To illustrate the ability of INDI to handle very large disturbances, a test flight was performed in which one tip propeller was configured to turn in the reverse direction. Not only does this tip propeller thereby create a negative lift and a very large roll moment, but it also acts as a variable disturbance as it is being changed by the controller. Fig. 8 shows the resulting perturbed take-off of the *NederDrone*. Although some initial oscillations can be seen during the first five seconds, the INDI controller keeps the *NederDrone* within acceptable attitudes and applies 100% actuator deflections to cope with the unexpected perturbation. Within three seconds it stabilized the platform and found the new equilibrium which requires a 25% roll command to compensate for the perturbation, while at the same time tracking aggressive outer-loop commands.

Results

The concept was built and tested in real flight. The wings are made of EPP cut with hot-wire and strengthened with dual carbon spars. Carbon ribs connect the spars to the motor mounts. Various parts like the motor mounts were built with the increasingly popular and powerful 3D printing technology [63]. To withstand the motor heat, the motor mounts were printed from a high-temperature resistant Ultimaker CPE + filament.

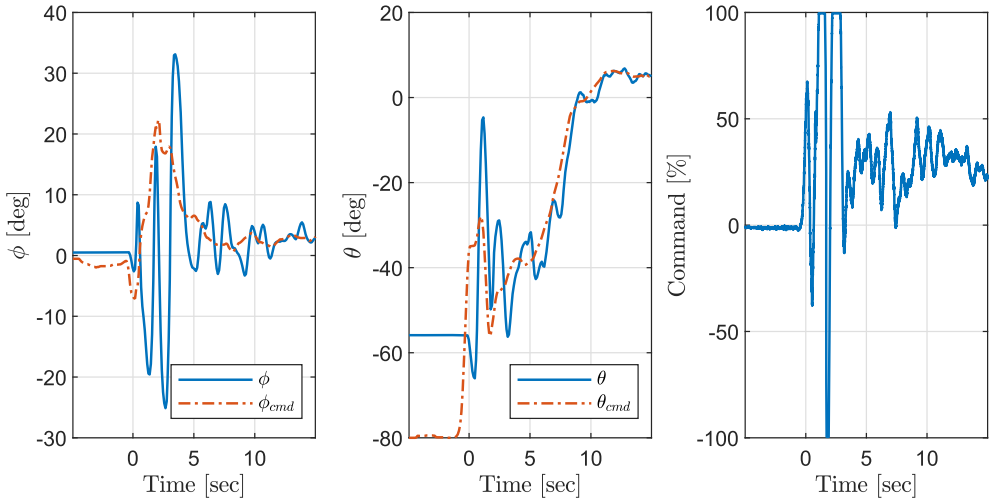

Fig. 8 – Time sequence of a take-off (t = 0) with a tip propeller spinning in reverse, causing a very large roll disturbance. The INDI controller needs 100% deflections to counteract the disturbance but finds the required trim command within seconds. Notice the 55° nose down θ when standing on the ground.

Please cite this article as: De Wagter C et al., The *NederDrone*: A hybrid lift, hybrid energy hydrogen UAV, International Journal of Hydrogen Energy, https://doi.org/10.1016/j.ijhydene.2021.02.053

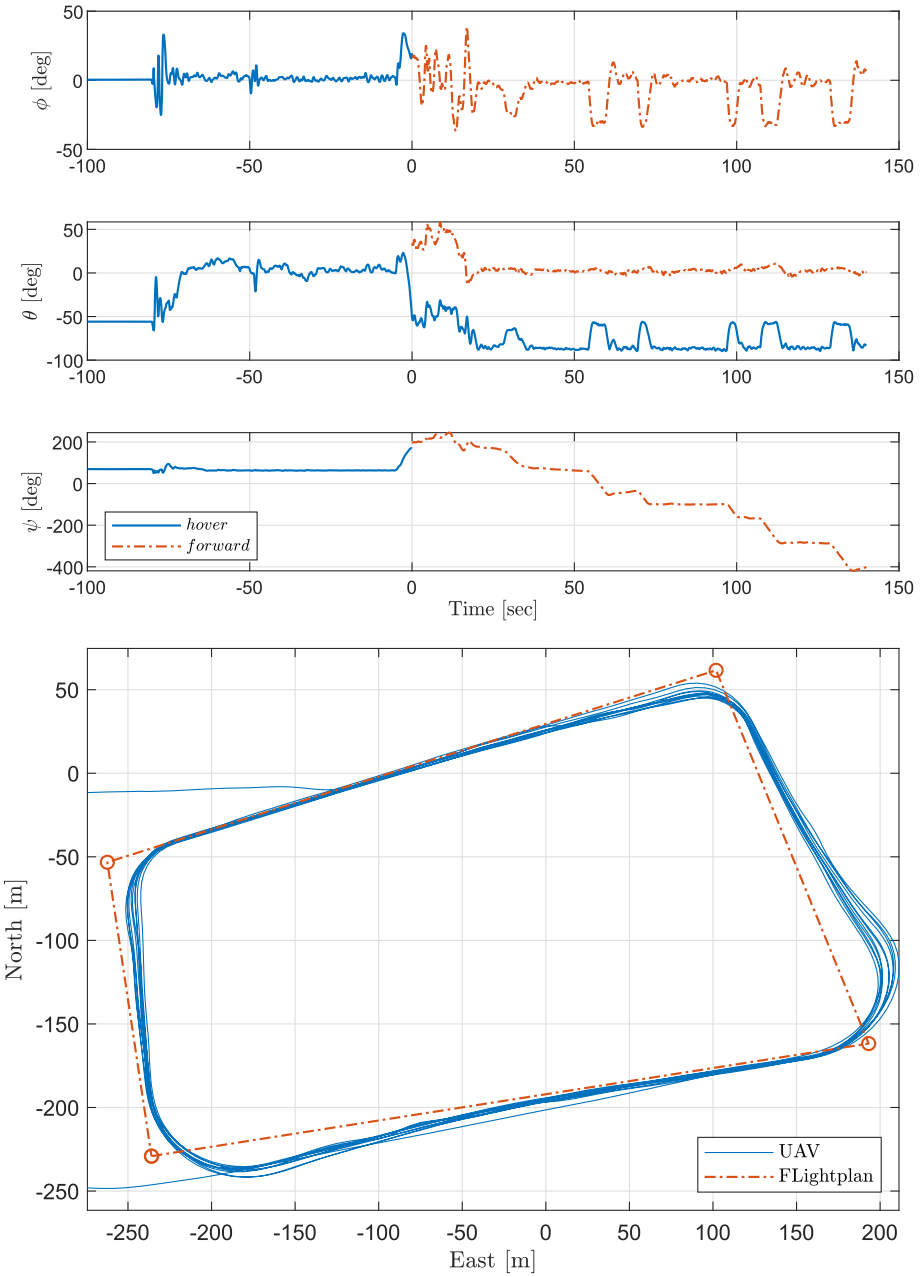

Fig. 9 – Test flight with take-off, hover, transition to forward and forward flight through a set of waypoints. The Euler angles in the plots swap from the hover frame to the forward frame upon transition. Onboard computations are performed in quaternions.

The autopilot software is the Paparazzi-UAV autopilot [64,65] project, which has support for various key features like low-level CAN drivers to INDI control implementations for hybrid aircraft, together with the ability to easily create custom modules to interface with the fuel-cell systems. The autopilot hardware is the Pixhawk PX4 *MBS-ENTB-24* board. The used motors are 12 T-Motor *MN3510-25-360* motors equipped with *APC 13x10* propellers. Servos are the water-proof *HS-5086WP* metal gear, micro digital waterproof servos. Telemetry is exchanged via the *HereLink* system.

Battery-only flight testing

Before flying with hydrogen, a mock-up hydrogen system was 3D printed and filled with batteries and metal to achieve the exact component weight. The mock-up cylinder was equipped with a 21 A h 1.865 kg 6S6P lithium-ion battery (*NCR18650GA*) to simulate the power delivered from the fuel-cell. This allowed it to safely fly over 30 min. A sample flight is shown in Fig. 9 in which the pitch angle on the ground, take-off, hover, transition, forward flight, and forward turns can be seen. Once the

Please cite this article as: De Wagter C et al., The *NederDrone*: A hybrid lift, hybrid energy hydrogen UAV, International Journal of Hydrogen Energy, https://doi.org/10.1016/j.ijhydene.2021.02.053

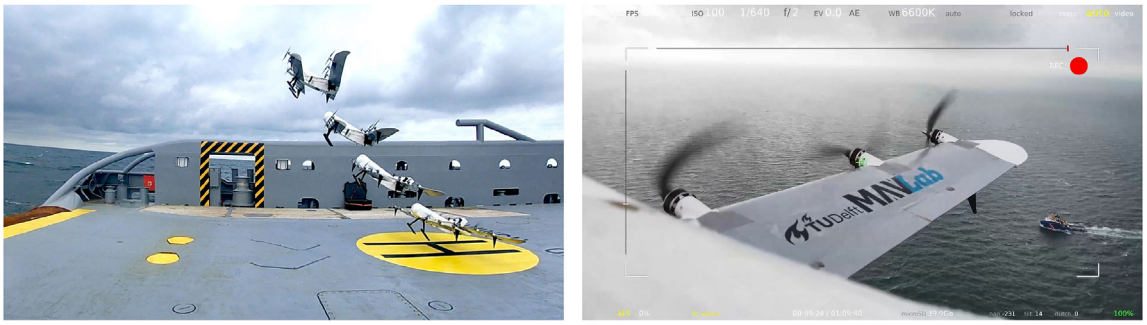

Fig. 10 – Hydrogen powered flight at sea departing from moving coast-guard vessel the *Guardian* with live-view.

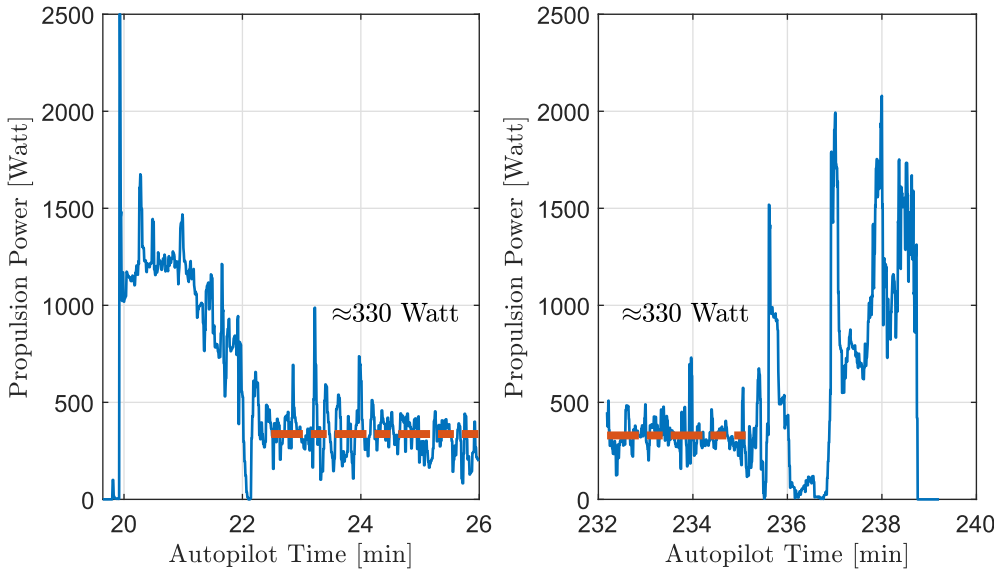

Fig. 11 – Flight power as reported by the ESC during the take-off and landing.

NederDrone with mock-up hydrogen components had flown dozens of flight hours successfully including many test flights from a ship, it was equipped with the hydrogen systems.

The first-ever hybrid lift hybrid energy hydrogen flight at sea

To demonstrate the capabilities of the *NederDrone* we performed a test flight at sea in real-world conditions. On September 30th, 2020, the *NederDrone* with fuel cell took off from a sailing coast guard ship in moderate wind conditions with 20 knots of wind. The flight lasted 3 h and 38 min. A composite image of the take-off is shown in Fig. 10a.

The onboard video of the pan-tilt HD camera protruding from the top of the *NederDrone* was streamed via the 2.4 GHz ISM-band HereLink data-link. A live video view of the *NederDrone* following the ship is shown in Fig. 10b. All battery-powered data-links and video systems were also charging from the hydrogen energy and stayed fully charged during the entire flight.

After landing, the empty cylinder can be replaced with a new full cylinder in seconds, before taking off again. The presented test flight does not push endurance to its limits. There was at least 20 min worth of hydrogen and 15 min of battery left after landing. All systems were running at full power and the weather was rough with 5 Beaufort (20 kt) wind and moderate turbulence. The propellers used during this flight were optimized for fast flight and not for maximum endurance. This illustrates that the hybrid lift hybrid power UAV called *NederDrone* is built for real-world operations and has considerable safety, performance, and energy margins.

Energy profile of the 3h38 flight

The hydrogen cylinder was filled with a pressure of 285 bar after settling at ambient temperature. It follows the inverse of the density profile from (2). Having reached the desired 3 flight hours, the flight was stopped at a remaining pressure

Please cite this article as: De Wagter C et al., The *NederDrone*: A hybrid lift, hybrid energy hydrogen UAV, International Journal of Hydrogen Energy, https://doi.org/10.1016/j.ijhydene.2021.02.053

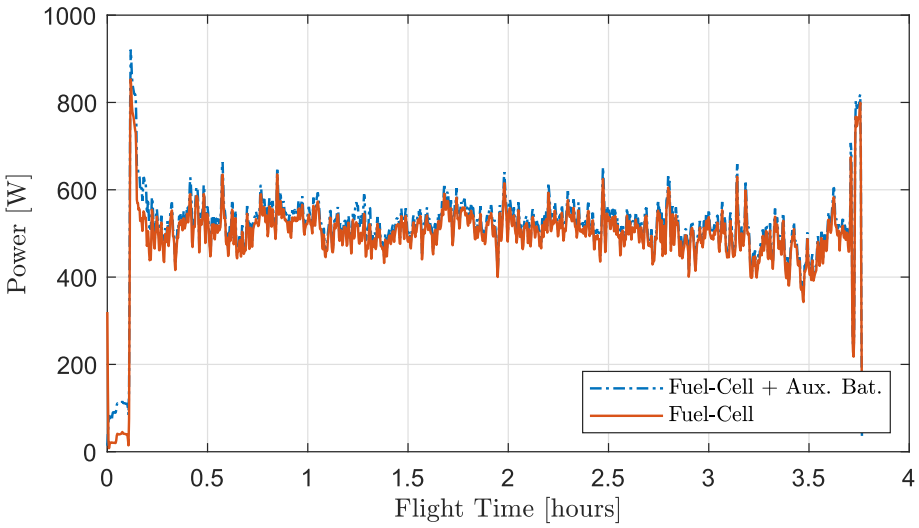

Fig. 12 – Power generation of the IE800 fuel-cell system.

of 20 bar, although previous tests proved that the *NederDrone* can continue to fly safely on battery power after complete depletion of the cylinder and shutdown of the fuel-cell.

During take-off and landing, lithium batteries provide the required extra power while the fuel-cell is running at maximum power. Fig. 11 shows the reported power used by the ESCs. This excludes the power used by the fuel-cell itself and its cooling, power losses in the long wires, power loss over the diodes, and power used by the payload and video link. The descend power becomes nearly zero at moments when the *NederDrone* is gliding in forward flight with the propellers windmilling. The climbing power (from 20 to 21 min) is about 1250 W during the angled take-off with the wings not stalled and thus significantly helping in lift production. The hover power required in the last phase of the landing while fighting turbulence with the wing stalled (238 min) consumed nearly 1500 W with peaks of over 2000 W. This is much more than the raw fuel-cell system can handle but is supplied from the high current rated lithium hover batteries with ease. Fig. 12 shows that the power delivered by the fuel-cell in those cases is about 800 W as by design.

The Intelligent Energy fuel-cell system comes with an auxiliary battery, which powers the fuel-cell electronics before the fuel-cell becomes active and helps in powering the system when more than 800 W is used. Fig. 12 shows that since most of the extra power is delivered by the much larger flight batteries, the auxiliary battery mainly serves to power the fuel-cell electronics and not the UAV, which results in nearly identical power with and without the auxiliary battery. While a power control loop could help to choose which battery is used or charged at each point in time, it would also add a lot of weight. The current fully passive setup performs as expected without any power electronics.

Two minutes after the take-off, the *NederDrone* transitions to forward flight and starts using much less power. The sum of the flight power, payload power, and fuel-cell systems (including cooling) power are an average of 550 W. After the take-off, the fuel-cell slowly re-charges the lithium batteries that were used during take-off. This means the hovering lithium batteries are fully charged before landing.

Discussion

Hydrogen is seen as a highly promising future fuel for aviation thanks to its high energy density. But the limited power that can be generated by fuel-cells limits the applicability. Furthermore, the onboard storage of pure hydrogen

Table 2 – Overview of the main advantages and disadvantages of the *NederDrone* concept.

	Advantage	Disadvantage
Propulsion	Re-use motors in forward and hover.	Reduced efficiency in hover.
Mechanical	Light: wings support the motors & props.	Transitioning 90° nose down.
Control	Redundant high authority control with excess power.	Need for high current batteries during hover.
Hybrid power	Passive parallel fuel-cell & batteries.	Power loss over diodes.
Redundancy	Redundant wiring, 12 props, 8 flaps.	Reduced propulsion efficiency.

Please cite this article as: De Wagter C et al., The *NederDrone*: A hybrid lift, hybrid energy hydrogen UAV, International Journal of Hydrogen Energy, https://doi.org/10.1016/j.ijhydene.2021.02.053

requires a pressure cylinder with a weight that is easily one-quarter of the vehicle weight and has shape constraints.

To allow the successful application of hydrogen in UAVs, it is important that the vehicle does not have severe operational limitations and it is essential that safety is guaranteed. This underlines the importance to find concepts that do not need very long runways but nevertheless fly fast and efficiently. At the same time, these platforms must be very safe as the consequences of accidents with onboard pressure cylinders filled with hydrogen can be significant. This requires platforms with redundant flight modes, redundant energy, and redundant control. The shape of the UAV can also play a big role in the protection of the cylinder. Light foam around the cylinder provides both an aerodynamic shape and a large crumple zone for low weight. By placing the sensitive high-pressure regulators backward in the middle of the vehicle, safety can be further increased. Last but not least, by having dual flight modes, an additional recovery mode is created in case of failure. When for instance aerodynamic actuators would fail, then the platform can return and land in hovering flight. If on the other hand, many motor controllers would fail, then the platform can still be flown in forward flight by exploiting the efficiency of its fixed-wings. This combined versatility and safety are expected to play an important role in the development of hydrogen-fuelled flight.

Conclusions

A novel hydrogen UAV was presented called the *NederDrone*[9]. It is a tail-sitter hybrid lift vehicle with tandem wings for forward flight, and 12 propellers for hover. The power comes from a PEM fuel-cell with hydrogen stored in a pressurized cylinder around which the UAV is optimized. The dual automotive CAN control bus, redundant power source, wiring, propulsion, dual flight modes, and model-less INDI control make the *NederDrone* particularly resilient to failures. The versatility and flight endurance of the *NederDrone* is shown with a 3h38 test flight at sea from a moving ship with 20 kt winds. The main advantages and disadvantages are summarized in Table 2.

Recommendations

Several aspects of the concept could be the subject of improvement. First of all, the presented flight time can be greatly extended by fitting larger amounts of hydrogen. The *NederDrone* was built with a 350 bar cylinder while 700 bar cylinders are available. This would require a new analysis of the safety aspects. Aerodynamically, airfoils with even smoother stall behavior but very low drag in forward flight should be developed to accommodate the specific needs of tail-sitter UAV. Electrically, a lot of power is lost in the cooling of the fuel-cell which could be done passively thanks to the incoming air. To reduce risks of overheating, this was not addressed in the present research as the temperature of the fuel-cell could not be measured in real-time. The control of the *NederDrone* is also the topic of future work. In hovering flight, the yaw axis of the *NederDrone* is controlled using the torque of the propellers and the induced flow of the propellers over the aerodynamic surfaces. Both moments are very small compared to pitch and roll moments, and this results in a lower performance of the yaw axis. Although the position of the UAV can be controlled well with the remaining roll and pitch, further work is recommended. Furthermore, the pitch angle of the *NederDrone* should not be allowed to move higher than about 20°—30° nose up in hover. Since during hover the *NederDrone* has a 90° higher pitch angle than during forward flight, pitching up even more will effectively place the fixed-wings in an inverted attitude (See Fig. 4 rotated 90° counterclockwise). While this is in itself not a problem, the flapping drag of the rotors while hovering backward bends the thrust vectors in the opposite direction than the direction of motion, which is such that it reduces the moment arm with respect to the center of gravity. In other words, since in hover, not all rotors are in the same plane, when translating in the positive X-direction (See Fig. 4), the maximally achievable pitch moment of the rotors is increased while in the negative X-direction the maximally achievable pitch moment is decreased. In both cases the forward flight stability of the wings cause a disturbing moment. While this can be solved by climbing or avoiding the situation altogether, further research is recommended on how to best use the aerodynamic actuators to overcome this situation. Finally, a lot of small improvements can still be made to the concept like retracting the landing gear in forward flight to reduce drag, reducing the small and underutilized auxiliary battery, and reducing the power loss over the diodes, which combined could result in additional improvements in performance and allow faster or longer operation in even tougher real-world conditions.

Declaration of competing interest

The authors declare that they have no known competing financial interests or personal relationships that could have appeared to influence the work reported in this paper.

Acknowledgements

The developments presented in this work would not have been possible without the support from the Royal Netherlands Navy and the Netherlands Coastguard.

[9] http://www.nederdrone.nl/.

Please cite this article as: De Wagter C et al., The *NederDrone*: A hybrid lift, hybrid energy hydrogen UAV, International Journal of Hydrogen Energy, https://doi.org/10.1016/j.ijhydene.2021.02.053

Appendix A. Cylinder Overview

An overview of the considered pressurized hydrogen cylinders is given in Table A.3.

Table A.3 – Cylinder Overview. Volume V, maximum pressure p, energy content E, weight W (regulator not included), hydrogen weight, specific weight percent of hydrogen, diameter D and length L.

	V [L]	p [bar]	E [Wh]	W [kg]	H_2 [g]	[Wh /kg]	WT% H_2	D [mm]	L [mm]
HES	2	350	1564	1.2	46.96	1303	3.91%	102	385
A-Series	2.5	350	1955	1.25	58.7	1564	4.70%	132	228
	3.5	350	2737	1.65	82.2	1659	4.98%	132	375
	5	350	3910	1.85	117.4	2113	4.44%	152	395
	9	350	7037	2.85	211.3	2469	7.41%	173	528
	12	350	9383	3.5	281.8	2681	8.05%	196	532
	20	350	15,638	7	469.6	2234	6.71%	230	665
Luxfer	3.8	379	3173	2.5	95.3	1269	3.81%		
	5.7	379	4759	3.3	142.9	1442	4.33%		
	6.8	300	4671	3.3	140.3	1415	4.25%	158	520
	7.6	379	6345	4.1	190.6	1548	4.65%		
	9	300	6182	4.3	185.7	1438	4.32%		
CTS	2	300	1374	1.23	41.3	1118	3.36%		
	3	300	2061	1.6	61.9	1288	3.87%		
	6	300	4121	2.9	123.8	1421	4.27%		
	6.8	300	4671	3.1	140.3	1507	4.52%	161	520
	7.2	300	4946	3.3	148.5	1499	4.50%	161	545
	9	300	6182	4.3	185.6	1438	4.32%		
	13	300	8930	5.3	268.2	1685	5.06%		
HES	2	300	1374	1.2	41.26	1145	3.44%	113	369
F-Series	3	300	2061	1.4	61.9	1472	4.42%	122	440
	6	300	4121	2.5	123.8	1649	4.95%	161	481
	6.8	300	4671	2.7	140.3	1730	5.20%	161	520
	7.2	300	4946	2.8	148.5	1766	5.30%	161	545
	9	300	6182	3.8	185.6	1627	4.89%	182	543

REFERENCES

[1] Pajares G. Overview and current status of remote sensing applications based on unmanned aerial vehicles (UAVs). Photogramm Eng Rem Sens 2015;81(4):281–330. https://doi.org/10.14358/pers.81.4.281.

[2] Boukoberine MN, Zhou Z, Benbouzid M. A critical review on unmanned aerial vehicles power supply and energy management: solutions, strategies, and prospects. Appl Energy 2019;255:113823. https://doi.org/10.1016/j.apenergy.2019.113823.

[3] Saeed AS, Younes AB, Cai C, Cai G. A survey of hybrid unmanned aerial vehicles. Prog Aero Sci 2018;98:91–105. https://doi.org/10.1016/j.paerosci.2018.03.007.

[4] Anderson SB. Historical overview of v/stol aircraft technology, techreport 19810010574. Moffett Field, CA, United States: NASA Ames Reseach Center; Mar. 1981. URL, https://ntrs.nasa.gov/search.jsp?R=19810010574.

[5] Hochstenbach M, Notteboom C, Theys B, De Schutter J. Design and control of an unmanned aerial vehicle for autonomous parcel delivery with transition from vertical take-off to forward flight -VertiKUL, a quadcopter tailsitter. Int J Micro Air Veh 2015;7(4):395–405. https://doi.org/10.1260/1756-8293.7.4.395.

[6] De Wagter C, Ruijsink R, Smeur EJJ, van Hecke KG, van Tienen F, van der Horst E, Remes BDW. Design, control, and visual navigation of the delftacopter vtol tail-sitter uav. J Field Robot 2018;35(6):937–60. https://doi.org/10.1002/rob.21789.

[7] Smeur EJ, Bronz M, de Croon GC. Incremental control and guidance of hybrid aircraft applied to a tailsitter unmanned air vehicle. J Guid Contr Dynam 2019:1. https://doi.org/10.2514/1.G004520.

[8] De Wagter C, Remes B, Ruijsink R, Van Tienen F, Van der Horst E. Design and testing of a vertical take-off and landing uav optimized for carrying a hydrogen fuel-cell with a pressure tank. Unmanned Syst 2020;8(4):279–85. https://doi.org/10.1142/S2301385020500223.

[9] Wang K, Ke Y, Chen BM. Autonomous reconfigurable hybrid tail-sitter UAV u-lion. Sci China Inf Sci 2017;(3):60. https://doi.org/10.1007/s11432-016-9002-x.

[10] Govdeli Y, Muzaffar SMB, Raj R, Elhadidi B, Kayacan E. Unsteady aerodynamic modeling and control of pusher and tilt-rotor quadplane configurations. Aero Sci Technol 2019;94:105421. https://doi.org/10.1016/j.ast.2019.105421.

[11] Hartmann P, Schütt M, Moormann D. Control of departure and approach maneuvers of tiltwing VTOL aircraft. In: AIAA guidance, navigation, and control conference. American Institute of Aeronautics and Astronautics; 2017. p. 1–18. https://doi.org/10.2514/6.2017-1914.

[12] Flores GR, Escareño J, Lozano R, Salazar S. Quad-tilting rotor convertible MAV: modeling and real-time hover flight

Please cite this article as: De Wagter C et al., The *NederDrone*: A hybrid lift, hybrid energy hydrogen UAV, International Journal of Hydrogen Energy, https://doi.org/10.1016/j.ijhydene.2021.02.053

control. J Intell Rob Syst 2011;65(1–4):457–71. https://doi.org/10.1007/s10846-011-9589-x.
[13] Pan Z, An L, Wen C. Recent advances in fuel cells based propulsion systems for unmanned aerial vehicles. Appl Energy 2019;240:473–85. https://doi.org/10.1016/j.apenergy.2019.02.079.
[14] Furrutter MK, Meyer J. Small fuel cell powering an unmanned aerial vehicle. In: AFRICON 2009. IEEE; 2009. p. 1–6. https://doi.org/10.1109/afrcon.2009.5308096.
[15] Kim T, Kwon S. Design and development of a fuel cell-powered small unmanned aircraft. Int J Hydrogen Energy 2012;37(1):615–22. https://doi.org/10.1016/j.ijhydene.2011.09.051.
[16] Lapeña-Rey N, Blanco J, Ferreyra E, Lemus J, Pereira S, Serrot E. A fuel cell powered unmanned aerial vehicle for low altitude surveillance missions. Int J Hydrogen Energy 2017;42(10):6926–40. https://doi.org/10.1016/j.ijhydene.2017.01.137.
[17] Özbek E, Yalin G, Ekici S, Karakoc TH. Evaluation of design methodology, limitations, and iterations of a hydrogen fuelled hybrid fuel cell mini UAV. Energy 2020;213:118757. https://doi.org/10.1016/j.energy.2020.118757.
[18] Banjong J, Therdthianwong A, Therdthianwong S, Yongprapat S, Wongyao N. High performance alkaline-acid direct glycerol fuel cells for portable power supplies via electrode structure design. Int J Hydrogen Energy 2020;45(3):2244–56. https://doi.org/10.1016/j.ijhydene.2019.11.041.
[19] Hordé T, Achard P, Metkemeijer R. PEMFC application for aviation: experimental and numerical study of sensitivity to altitude. Int J Hydrogen Energy 2012;37(14):10818–29. https://doi.org/10.1016/j.ijhydene.2012.04.085.
[20] Pareta M, Choudhury SR, Somaiah B, Rangarajan J, Matre N, Palande J. Methanol reformer integrated phosphoric acid fuel cell (PAFC) based compact plant for field deployment. Int J Hydrogen Energy 2011;36(22):14771–8. https://doi.org/10.1016/j.ijhydene.2011.03.044.
[21] Yu F, Han T, Wang Z, Xie Y, Wu Y, Jin Y, Yang N, Xiao J, Kawi S. Recent progress in direct carbon solid oxide fuel cell: advanced anode catalysts, diversified carbon fuels, and heat management. Int J Hydrogen Energy 2021. https://doi.org/10.1016/j.ijhydene.2020.10.259.
[22] Koomson S, Lee C-G. Lifetime expectancy of molten carbonate fuel cells: Part i. effect of temperature on the voltage and electrolyte reduction rates. Int J Hydrogen Energy 2021. https://doi.org/10.1016/j.ijhydene.2020.07.218.
[23] Chen X, Li T, Shen J, Hu Z. From structures, packaging to application: a system-level review for micro direct methanol fuel cell. Renew Sustain Energy Rev 2017;80:669–78. https://doi.org/10.1016/j.rser.2017.05.272.
[24] Kim T. NaBH4 (sodium borohydride) hydrogen generator with a volume-exchange fuel tank for small unmanned aerial vehicles powered by a PEM (proton exchange membrane) fuel cell. Energy 2014;69:721–7. https://doi.org/10.1016/j.energy.2014.03.066.
[25] Schlapbach L, Züttel A. Hydrogen-storage materials for mobile applications. In: Materials for sustainable energy. UK: Co-Published with Macmillan Publishers Ltd; 2010. p. 265–70. https://doi.org/10.1142/9789814317665_0038.
[26] Luo Y, Shi Y, Cai N. Bridging a bi-directional connection between electricity and fuels in hybrid multienergy systems. In: Hybrid systems and multi-energy networks for the future energy internet. Elsevier; 2021. p. 41–84. https://doi.org/10.1016/b978-0-12-819184-2.00003-1.
[27] Zhao J, Sheng Y-J, Cai Y-L, Teng Y-L, Wang L, Ping C, Shen M, Dong B-X. Efficiently generating COx-free hydrogen by mechanochemical reaction between alkali hydrides and carbon dioxide. Int J Hydrogen Energy 2019;44(33):18159–68. https://doi.org/10.1016/j.ijhydene.2019.05.134.
[28] Troncoso E, Lapeña-Rey N, Valero O. Solar-powered hydrogen refuelling station for unmanned aerial vehicles: design and initial AC test results. Int J Hydrogen Energy 2014;39(4):1841–55. https://doi.org/10.1016/j.ijhydene.2013.11.064.
[29] Xu D, Zhang H, Ye W. Hydrogen generation from hydrolysis of alkaline sodium borohydride solution using pt/c catalyst. Catal Commun 2007;8(11):1767–71. https://doi.org/10.1016/j.catcom.2007.02.028.
[30] Keçeli E, Özkar S. Ruthenium(III) acetylacetonate: a homogeneous catalyst in the hydrolysis of sodium borohydride. J Mol Catal A Chem 2008;286(1–2):87–91. https://doi.org/10.1016/j.molcata.2008.02.008.
[31] Liao J, Feng Y, Lin W, Su X, Ji S, Li L, Zhang W, Pollet BG, Li H. CuO–NiO/co3o4 hybrid nanoplates as highly active catalyst for ammonia borane hydrolysis. Int J Hydrogen Energy 2020;45(15):8168–76. https://doi.org/10.1016/j.ijhydene.2020.01.155.
[32] González EL, Cuesta JS, Fernandez FJV, Llerena FI, Carlini MAR, Bordons C, Hernandez E, Elfes A. Experimental evaluation of a passive fuel cell/battery hybrid power system for an unmanned ground vehicle. Int J Hydrogen Energy 2019;44(25):12772–82. https://doi.org/10.1016/j.ijhydene.2018.10.107.
[33] Herwerth C, Chiang C, Ko A, Matsuyama S, Choi SB, Mirmirani M, Gamble D, Paul R, Sanchez V, Arena A, Koschany A, Gu G, Wankewycz T, Jin P. Development of a small long endurance hybrid PEM fuel cell powered UAV. In: SAE technical paper series. SAE International; 2007. https://doi.org/10.4271/2007-01-3930.
[34] Gong A, Verstraete D. Fuel cell propulsion in small fixed-wing unmanned aerial vehicles: current status and research needs. Int J Hydrogen Energy 2017;42(33):21311–33. https://doi.org/10.1016/j.ijhydene.2017.06.148.
[35] Bradley T, Moffitt B, Parekh D, Mavris D. Flight test results for a fuel cell unmanned aerial vehicle. In: 45th AIAA aerospace sciences meeting and exhibit. American Institute of Aeronautics and Astronautics; 2007. p. 1–8. https://doi.org/10.2514/6.2007-32.
[36] Gadalla M, Zafar S. Analysis of a hydrogen fuel cell-pv power system for small uav. Int J Hydrogen Energy 2016;41(15):6422–32. https://doi.org/10.1016/j.ijhydene.2016.02.129.
[37] Gavrilovic N, Vincekovic D, Moschetta J-M. A long range fuel cell/soaring uav system for crossing the atlantic ocean. In: Campoy P, editor. 11th international micro air vehicle competition and conference, madrid, Spain. IMAV; 2019. p. 121–31. URL, http://www.imavs.org/pdf/imav.2019.16.
[38] Rottmayer M, Miller R. Fuel cell hybrid power system development for extended endurance SUAS applications. In: AIAA centennial of naval aviation forum "100 Years of achievement and progress". American Institute of Aeronautics and Astronautics; 2011. p. 1–3. https://doi.org/10.2514/6.2011-6976.
[39] Stephens IEL, Rossmeisl J, Chorkendorff I. Toward sustainable fuel cells. Science 2016;354(6318):1378–9. https://doi.org/10.1126/science.aal3303.
[40] Wang B, Zhao D, Li W, Wang Z, Huang Y, You Y, Becker S. Current technologies and challenges of applying fuel cell hybrid propulsion systems in unmanned aerial vehicles. Prog Aero Sci 2020;116:100620. https://doi.org/10.1016/j.paerosci.2020.100620.
[41] Kaya N, Turan Önder, Karakoç TH, Midilli A. Parametric study of exergetic sustainability performances of a high altitude long endurance unmanned air vehicle using

Please cite this article as: De Wagter C et al., The *NederDrone*: A hybrid lift, hybrid energy hydrogen UAV, International Journal of Hydrogen Energy, https://doi.org/10.1016/j.ijhydene.2021.02.053

hydrogen fuel. Int J Hydrogen Energy 2016;41(19):8323–36. https://doi.org/10.1016/j.ijhydene.2015.09.007.
[42] Kim J, Kim D-M, Kim S-Y, Nam SW, Kim T. Humidification of polymer electrolyte membrane fuel cell using short circuit control for unmanned aerial vehicle applications. Int J Hydrogen Energy 2014;39(15):7925–30. https://doi.org/10.1016/j.ijhydene.2014.03.012.
[43] Züttel A. Hydrogen storage methods. Naturwissenschaften 2004;91(4):157–72. https://doi.org/10.1007/s00114-004-0516-x.
[44] Kim K, Kim T, Lee K, Kwon S. Fuel cell system with sodium borohydride as hydrogen source for unmanned aerial vehicles. J Power Sources 2011;196(21):9069–75. https://doi.org/10.1016/j.jpowsour.2011.01.038.
[45] Boran A, Erkan S, Eroglu I. Hydrogen generation from solid state NaBH4 by using FeCl3 catalyst for portable proton exchange membrane fuel cell applications. Int J Hydrogen Energy 2019;44(34):18915–26. https://doi.org/10.1016/j.ijhydene.2018.11.033.
[46] Y. Lee, E.-T. Park, J. Jeong, H. Shi, J. Kim, B.-S. Kang, W. Song, Weight optimization of hydrogen storage vessels for quadcopter UAV using genetic algorithm, Int J Hydrogen Energy:10.1016/j.ijhydene.2020.09.014.
[47] Troncoso E, Lapeña-Rey N, Valero O. Off-grid test results of a solar-powered hydrogen refuelling station for fuel cell powered unmanned aerial vehicles. Int J Hydrogen Energy 2014;39(21):11267–78. https://doi.org/10.1016/j.ijhydene.2014.04.192.
[48] Molnarne M, Schroeder V. Hazardous properties of hydrogen and hydrogen containing fuel gases. Process Saf Environ Protect 2019;130:1–5. https://doi.org/10.1016/j.psep.2019.07.012.
[49] Mashayekhi M. Prediction of all-steel cng cylinders fracture in impact by using damage mechanics approach. Sci Iran 2014;21(3):609–19. URL, http://scientiairanica.sharif.edu/article_3500.html.
[50] Bertin M, Halm D, Magneville B, Renard J, Saffré P, Villalonga S. One year osirhys iv project synthesis: mechanical behaviour of 700 bar type iv high pressure vessel code qualification. In: HAL-00801409; 2012. p. 1–8. URL, https://hal.archives-ouvertes.fr/hal-00801409.
[51] Mitsuishi H, Oshino K, Watanabe S. Dynamic crush test on hydrogen pressurized cylinder, Disp 2000. 2005. p. 1–50. URL, https://h2tools.org/sites/default/files/2019-09/310001. pdf.
[52] Molkov V, Kashkarov S. Blast wave from a high-pressure gas tank rupture in a fire: stand-alone and under-vehicle hydrogen tanks. Int J Hydrogen Energy 2015;40(36):12581–603. https://doi.org/10.1016/j.ijhydene.2015.07.001.
[53] Schmidt LV. Introduction to aircraft flight dynamics. American Institute of Aeronautics and Astronautics; 1998. https://doi.org/10.2514/4.862052.
[54] Vermeer L. A review of wind turbine wake research at TU delft. In: 20th 2001 ASME wind energy symposium. American Institute of Aeronautics and Astronautics; 2001. p. 1–11. https://doi.org/10.2514/6.2001-30.
[55] F. Aymen, Internal fuzzy hybrid charger system for a hybrid electrical vehicle, J Energy Resour Technol 140 (1). doi:10.1115/1.4037352.
[56] Martinez-Heredia JM, Colodro F, Mora-Jimenez JL, Remujo A, Soriano J, Esteban S. Development of GaN technology-based DC/DC converter for hybrid UAV. IEEE Access 2020;8:88014–25. https://doi.org/10.1109/access.2020.2992913.
[57] Sparks J. Low cost technologies for aerospace applications. Microprocess Microsyst 1997;20(8):449–54. https://doi.org/10.1016/S0141-9331(96)01109-X.
[58] Ravi N, El-Sharkawy M. Integration of UAVs with real time operating systems using UAVCAN. In: 2019 IEEE 10th annual ubiquitous computing, electronics & mobile communication conference (UEMCON). IEEE; 2019. p. 600–5. https://doi.org/10.1109/uemcon47517.2019.8993011.
[59] Smeur EJJ, Chu QP, de Croon GCHE. Adaptive incremental nonlinear dynamic inversion for attitude control of micro aerial vehicles. J Guid Contr Dynam 2016;39(3):450–61. https://doi.org/10.2514/1.G001490.
[60] Smeur E, de Croon G, Chu Q. Cascaded incremental nonlinear dynamic inversion for mav disturbance rejection. Contr Eng Pract 2018;73:79–90. https://doi.org/10.1016/j.conengprac.2018.01.003.
[61] Smeur EJJ, E de Croon de GCH, Chu Q. Gust disturbance alleviation with incremental nonlinear dynamic inversion. In: International conference on intelligent robots and systems (IROS). IEEE/RSJ, IEEE, Daejeon, South Korea; 2016. p. 5626–31. https://doi.org/10.1109/IROS.2016.7759827.
[62] Preumont A. Vibration control of active structures. Springer International Publishing; 2018. https://doi.org/10.1007/978-3-319-72296-2.
[63] Goh G, Agarwala S, Goh G, Dikshit V, Sing S, Yeong W. Additive manufacturing in unmanned aerial vehicles (UAVs): challenges and potential. Aero Sci Technol 2017;63:140–51. https://doi.org/10.1016/j.ast.2016.12.019.
[64] Brisset P, Drouin A, Gorraz M, Huard P-S, Tyler J. The paparazzi solution. In: MAV 2006, 2nd US-European competition and workshop on micro air vehicles, sandestin, United States; 2006. p. 1–15. URL, https://hal-enac.archives-ouvertes.fr/hal-01004157.
[65] Gati B. Open source autopilot for academic research-the paparazzi system. In: American control conference (ACC), 2013. Washington, DC: IEEE; 2013. p. 1478–81. https://doi.org/10.1109/ACC.2013.6580045.

Please cite this article as: De Wagter C et al., The *NederDrone*: A hybrid lift, hybrid energy hydrogen UAV, International Journal of Hydrogen Energy, https://doi.org/10.1016/j.ijhydene.2021.02.053